Neural Correlations across Mice during Spontaneous and Task-Related Behaviors

Daiyao Yi
Department of Electrical and Computer Engineering
University of Florida
Gainesville, USA
yidaiyao@ufl.edu

Shreya Saxena
Department of Electrical and Computer Engineering
University of Florida
Gainesville, USA
shreya.saxena@ufl.edu

2023 11th International IEEE/EMBS Conference on Neural Engineering (NER) | 978-1-6654-6292-1/23/$31.00 ©2023 IEEE | DOI: 10.1109/NER52421.2023.10123873

***Abstract*—While the neural commonalities as subjects perform similar task-related behaviors has been previously examined, it is very difficult to ascertain the neural commonalities for spontaneous, task-unrelated behaviors such as grooming. As our ability to record high-dimensional naturalistic behavioral and corresponding neural data increases, we can now try to understand the relationship between different subjects performing spontaneous behaviors that occur rarely in time. Here, we first apply novel machine learning techniques to behavioral video data from four head-fixed mice as they perform a self-initiated decision-making task while their neural activity is recorded using widefield calcium imaging. Across mice, we automatically identify spontaneous behaviors such as grooming and task-related behaviors such as lever pulls. Next, we explore the commonalities between the neural activity of different mice as they perform these tasks by transforming the neural activity into a common subspace, using Multidimensional Canonical Correlation Analysis (MCCA). Finally, we compare the commonalities across different trials in the same subject to those across subjects for different types of behaviors, and find that many recorded brain regions display high levels of correlation for spontaneous behaviors such as grooming. The combined behavioral and neural analysis methods in this paper provide an understanding of how similarly different animals perform innate behaviors.**

***Index Terms*—Canonical Correlation Analysis, Neural Activity, Across-subject analysis**

I. Introduction

It remains under-explored how neural activity changes across different animals from the same species while performing the same tasks. Recovering commonalities in neural activity across different trials and conditions has been demonstrated in previous studies [1]. Here we explore the neural activity correlations while the subjects perform similar spontaneous behaviors vs. task-related behaviors.

To obtain neural activity when different animals are performing similar behaviors, the first thing to do is to identify periods of time when the behavior is similar across animals. Here, we model high-dimensional video behavioral recordings into a lower-dimensional space in a way that captures a large percentage of the variance. To achieve this, researchers in this field have designed several methods. Pose estimation methods, for example, DeepLabCut (DLC), LEAP and AlphaTracker, [2]–[4], etc, are popular supervised methods to study animal behavior. Although these methods work well in across-subject settings, they may be missing key information in the behavioral videos, for example, the face moving, the whiskers, and small muscle movements. The unsupervised methods for behavioral feature extractions can address questions that require characterizing these key pieces of information. For example, MoSeq analyzes the behaviors by directly applying Principal Component Analysis (PCA) to the behavioral videos [5], [6]. Similarly, Behavenet uses non-linear autoencoders to learn the representations from the videos [7]. However, both of those models failed in generating interpretable latent variables. In addition to that, those methods failed to capture the same behavior while distinguishing different animals in the across-subject settings. Therefore, here, we apply CS-VAE [8] to behavioral data across mice performing a delayed self-initiated two-alternative forced choice (2AFC) task. CS-VAE is inspired from MSPS-VAE [9], but is more robust for a continuously varying and unknown number of sessions or subjects.

In addition to the behaviors, the neural activity has been simultaneously recorded and preprocessed by LocaNMF [10], which enables efficient dimensionality reduction of the neural activity while keeping region-based information, thus allowing us to capture a high amount of variance in the neural data across subjects. CCA has been widely adopted in many studies related to neural signal processing [11], [12]. Here, we perform the alignment for multi-subject neural activities using Multidimensional Canonical Correlation Analysis (MCCA). The alignment is achieved by linearly projecting the neural activity into the same (common) feature space.

The overall workflow is shown in Fig. 1A. In this work, we explore the cross-subject neural relationships for different brain regions. We first explain the workflow for selecting similar behavior in multiple subjects and across a single subject. Then, we introduce the mathematical details of MCCA and how it can be used to align the neural activity for different subjects performing similar behaviors. Next, we compare the neural correlations in across-subject settings and in same-subject settings. Finally, we discuss future work.

II. Methods

In this section, we first introduce the experimental data used in this work. Then, we give a brief overview of the model that we applied to generate the behavioral latent variables and the

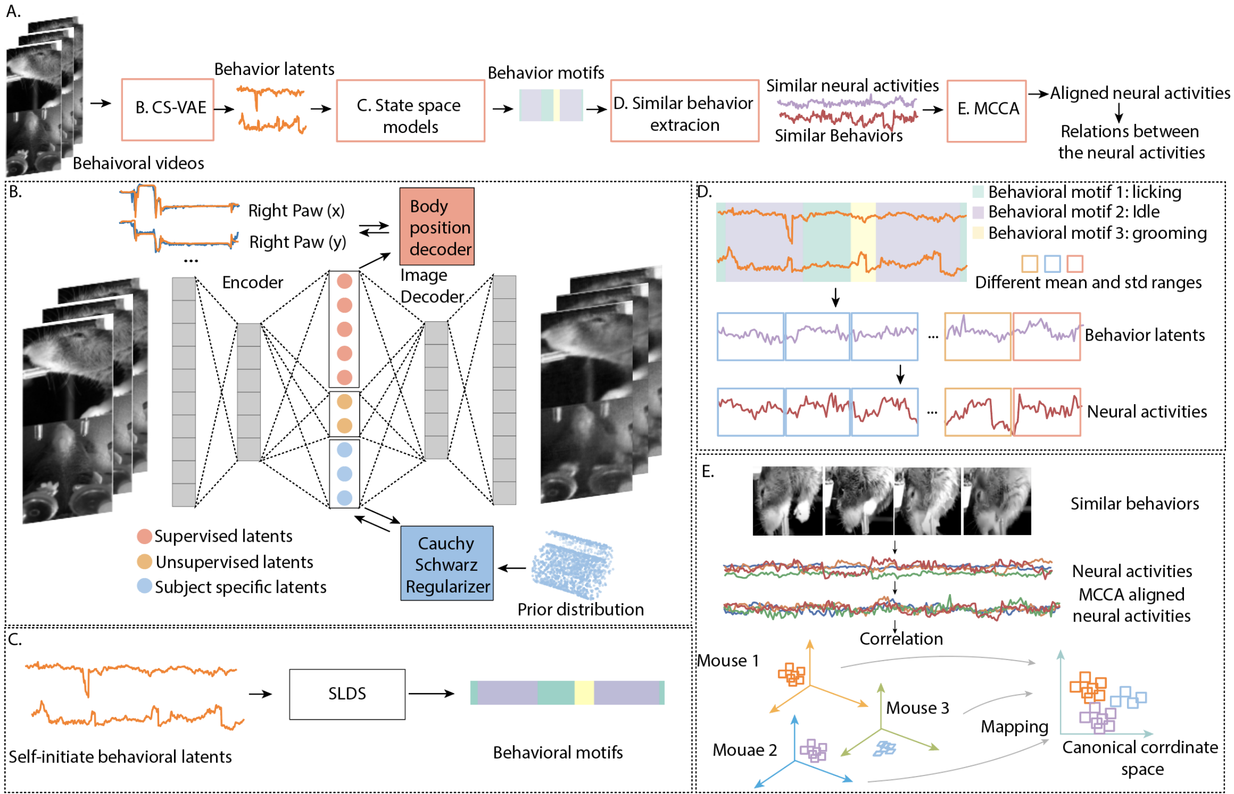

Fig. 1. Overview of the model A. The overall workflow for comparing the neural activities for different subjects performing similar spontaneous behaviors: First, the behavioral videos are being encoded into behavior latents by CS-VAE. Then, the behavior latents would be clustered into different motifs. After that, similar behaviors are grouped based on their mean and standard deviation values. We can therefore obtain the corresponding neural activities. Finally, the neural activities from different subjects are aligned using the MCCA. B. CS-VAE structure: The video data is being encoded into three latent spaces: (1) the supervised latents decode the labeled body positions, (2) the unsupervised latents model the subject's behavior that is not explained by the supervised latents, and (3) the constrained subspace latents model the features relating to multi-subject. C. Behavioral motif generation: The unsupervised latents from part B are the observation of the SLDS model. The behavioral motifs are the outputs of the state space model. D. Behavior latents are cut into small fragments. Similar behavior fragments are grouped together based on their mean and standard deviation values. The corresponding neural activities are obtained based on the grouping results of the behavior. E. Neural activities are being aligned using MCCA. MCCA aligns the neural activities from different subjects by mapping them into the same feature spaces.

corresponding behavioral motifs. Finally, we detail MCCA that we used for neural dynamic alignment.

A. *Experimental Methods*

In our work, we explored a subset of the behavioral dataset detailed in Musall et al., 2019 [13]. Here, head-fixed mice perform a self-initiated visual discrimination task. Each task is initiated by the mouse pressing a lever, followed by a visual stimulus that is displayed towards the left or the right. The spouts on both sides come inwards after a short delay, and if the mouse licks the correct spout that corresponds to the direction of the visual stimulus, a water reward is provided. The dataset has the task-related actions that are annotated automatically with trial-markers based on various sensors, such as force sensors on the levers. Beyond these task-related actions, the mice also perform other spontaneous, task-unrelated actions, such as grooming, raising a paw, whisking, etc. The behaviors of the mice were recorded from two views (face and body). During the tasks, the neural activity across the entire mouse dorsal cortex was also recorded in the form of widefield calcium imaging. Here, we work with data from four mice with 388 trials for each mouse. Each trial lasts for 6.3 seconds. The spatial resolution for the widefield calcium imaging was $20\mu m$ per pixel and the total field of view was $12.5 \times 10.5mm^2$. The recording runs at 60 frames per second. Further recording details can be found in [13], with the preprocessing details in [10].

B. *Constrained-Subspace Variational Autoencoder (CS-VAE)*

CS-VAE is a semi-supervised VAE that produces interpretable latent variables for multi-subjects datasets or datasets with continuously varying backgrounds, etc. It does this by partitioning the latent into three subspaces: supervised space, unsupervised space, and subject-specific space, as shown in Fig 1B. The supervised latent encodes the positions of the body parts, such as paws, nose, etc., and also the position of the various equipment in our field of view, such as levers, spouts, etc. The positions were obtained using DeepLabCut (DLC) [14]. The unsupervised latents capture the time-varying movement that has not been encoded by the supervised latent.

In our study, the unsupervised information is the 'jaw movement' and the 'chest movement'. The subject-specific latents capture the appearance of each subject, such as the size of the eye, the color of the fur, the place where the head is fixed, etc. This is achieved by regularizing the latent space with the Cauchy-Schwarz divergence. With this regularization, the latent in this subspace is constrained to a pre-defined prior distribution. By properly choosing the prior distribution, subjects from different groups can be automatically separated in this latent space, so that the difference across them can be captured. In addition, the separation of each latent is achieved by ensuring orthogonality between them.

The model includes three parts: the encoder, the latent subspaces, and the decoder. After the image goes through the encoder with five convolutional layers in sequence, it is encoded into the lower dimensional subspaces that are described above. To ensure the latent that we get has the ability in capturing the information in the image, they would then go into the following decoder which is symmetric to the encoder. Details about the model and mathematical underpinnings can be found in [8].

C. Behavioral motif generation

To obtain the behavioral motifs for behaviors that are largely self-initiated, we used the unsupervised latents from the CS-VAE model. We modeled the unsupervised latents as observations in a switched linear dynamical system (SLDS) and generated the behavioral motifs (Fig. 1C). An SLDS consists of three states: a discrete latent state $z_t \in \{1, 2, ..K\}$, a continuous latent state $x_t \in \mathbb{R}^M$, and the observation $y_t \in \mathbb{R}^N$. Here, $t = 1, 2, 3, .., T$ is the time step, T is the length of the input signal; K is the number of discrete states; M is the number of latent dimensions; N is the observation dimensions. The discrete latent state z_t follows the Markovian dynamics with the state transition matrix expressed as:

$$Q_{i,j} = P(z_t = j|z_{t-1} = i) \quad (1)$$

The continuous latent state x_t has the following linear dynamical relations that are determined by z_t.

$$x_{t+1} = A_{z_{t+1}} x_t + V_{z_{t+1}} u_t + b_{z_{t+1}} + w_t \quad (2)$$

Here, $A_{z_{t+1}}$ is the dynamic matrix at state z_{t+1}; u_t is the input at time t, with $V_{z_{t+1}}$ being the control matrix; $b_{z_{t+1}}$ is the offset vector and w_t being the noise which is generally the zero mean Gaussian. Here, our observation model is in Gaussian case; therefore, the observation y_t is expressed as:

$$y_t = C_{z_t} x_t + F_{z_t} u_t + d_{z_t} + v_t \quad (3)$$

Here, C_{z_t} is the measurement matrix at state z_t; F_{z_t} is the feed-through matrix which directly feed the input into the observation; d_{z_t} is the offset vector and v_t is the noise. Here the update was accomplished by the Expectation-Maximization (EM) algorithm. In the E-step, the model updates the hyperparameters. In the M-step, the log-likelihood in Eq.3 is being maximized.

D. Behavior selection

Although the behavioral features generated from Sec II-B succeed in capturing similar spontaneous behaviors across different animals, the behavior from the same behavioral motifs can vary substantially. For example, for the raising paw motif, the continuous moving up the paws could be grooming or other complex behaviors. To address this problem, we first cut the behavior from the same motif into small chunks, in which we calculated the corresponding mean and standard deviation of the behavioral latents. Finally, we compared those values and kept the chunks that have similar mean and standard deviations within and across animals as shown in Fig. 1D. The above steps were performed for all behavioral motifs considered in this study.

In addition to the spontaneous behaviors stated above, we also selected an 'idle' behavior where the mouse is not seen to be moving much, and one task-related behavior, namely a 'lever pull' behavior that is used to indicate the initiating of each task (Fig. 2A).

E. Multidimensional Canonical Correlation Analysis (MCCA) for neural signal alignment

Here, we adopt the assumptions in Safaie et al. [1] that when the animals perform the same actions, the neural latent will share similar dynamics. We employ MCCA to align the high-dimensional neural activity across multiple subjects [15]. CCA is a linear model for finding the relationships between two datasets by identifying a common lower dimensional space. MCCA, as its name implies, is the model for finding the a common lower-dimensional space across multiple datasets. To do this, CCA or MCCA projects the datasets onto a canonical coordinate space that maximizes correlations between them (Fig. 1E).

In our work, after extracting similar behaviors chunks from different individuals (see Sec II-D), we then extracted the corresponding neural activity for each subject. To smooth away the discreteness of the neural activity chunks, we shuffled the chunks before concatenating them together. After that, we performed the MCCA for all four subjects on each brain region. For each brain region, we choose the four sets of neural activities being the same length d, $X1 = \{x1_1, x1_2, ..., x1_n\} \in R^{n\times d}$, $X2 = \{x2_1, x2_2, ..., x2_n\} \in R^{m\times d}$, $X3 = \{x3_1, x3_2, ..., x3_n\} \in R^{k\times d}$, and $X1 = \{x1_1, x1_2, ..., x1_n\} \in R^{l\times d}$. Here, we choose the minimum number of region dimensionality in all of the four subjects as the dimension of canonical coordinate space, $minimum\{n, m, k, l\}$, and is annotated as j. For each dimension, define the projection weights for each dataset as $a_j = \{a_{j1}, a_{j2}, .., a_{jn}\}$, $b_j = \{b_{j1}, b_{j2}, .., b_{jn}\}$, $c_j = \{c_{j1}, c_{j2}, .., c_{jn}\}$, and $d_j = \{d_{j1}, d_{j2}, .., d_{jn}\}$. The resulting projected datasets are now d-dimensional arrays: $u1_j = \langle a_j, X1\rangle$, $u2_j = \langle b_j, X2\rangle$, $u3_j = \langle c_j, X3\rangle$, and $u4_j = \langle d_j, X4\rangle$. For each of the coordinate spaces, the objective functions can be written as:

$$\rho_j = \frac{\langle u1_j, u2_j, u3_j, u4_j\rangle}{\|u1_j\|\|u2_j\|\|u3_j\|\|u4_j\|} \quad (4)$$

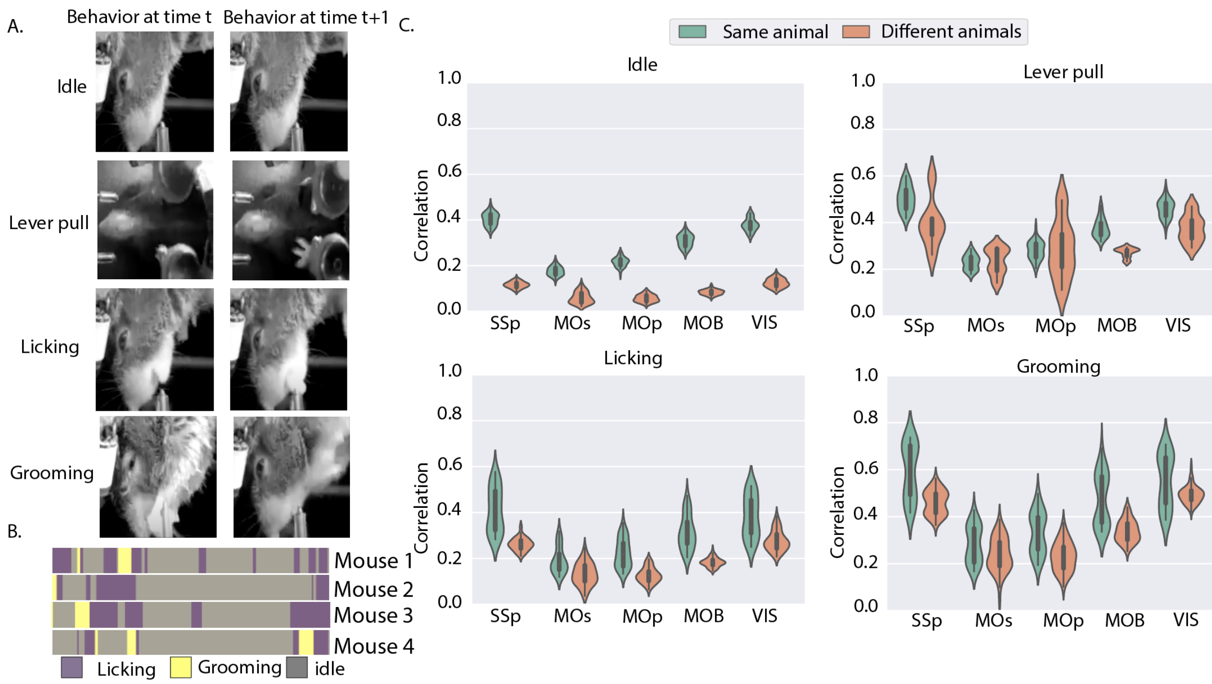

Fig. 2. A. Example screenshot of each behavior for one of the subjects B. One example ethogram of the self-initiated behavior for each mouse. Each behavior happens at approximately the same rate C. Correlation score for behavioral-based aligned neural activity. The grooming behavior has higher neural correlation scores for cross-subjects than other behaviors.

Generally, for each pair of canonical components, the above equation is solved iteratively to find the best projects that can maximize the correlation. During training, the orthogonality between each canonical component is constrained. In our experiment, we calculated the across-subject correlations for each obtained CCs and kept the highest correlation value for each pair, here termed ρ_1 (Equation 4). We performed the above task for each brain region. In addition, we shuffled the chunks ten times and repeated the above steps.

We also calculated the canonical component for the same subject having similar behaviors. We applied the same methods as stated above to find similar behavior components and the corresponding neural activities. We divided the obtained neural activities into two parts with the same length and performed the CCA on those two signals. We calculated the correlation between the first two canonical correlation axes as the baseline.

III. Results

A. Behavioral motifs across subjects

The motif generation results are detailed in [8]. As seen in the ethograms in Fig. 2, with the CS-VAE latents as the observation to the SLDS model, it captures common states across different subjects. Here, we have three motifs, licking, idle, and grooming. These states also occur with a very similar frequency across mice with the mean frequency being 0.22 ± 0.10, 0.72 ± 0.08, and 0.06 ± 0.04. Example images for each behavior are shown in Fig. 2. In addition to that, we also add the task-related motif, lever pull, which annotated using a force sensor on the levers. This behavior happens every trial and is for initiating the task.

B. Across-subject commonalities in neural activity

We compare the commonalities across subjects to the commonalities for two random instances of the behavior performed by the same subject by plotting the correlation scores in the form of violin graphs. For the same subject. The 'same subject' commonality provides a baseline for the across-subject correlations. As previously described, the shuffled tasks were performed 10 times for each time calculating the correlation value. There are 40 points contained in each violin plot. For the cross-subjects, we calculate the correlation values in a pairwise manner, i.e., for two subjects at a time, with the neural activity pre-aligned for all four subjects. We also performed the shuffling task; thus, there are 60 points in each violin plot.

In Figure 2, we see that for the idle behavior, the neural correlation across mice is much lower than the correlation within the same mouse; however, this does not hold for the task related behaviors such as lever pull and licking, or the spontaneous behaviors such as grooming. For the grooming behavior, the neural correlations within and across subjects are much higher than for the idle behaviors, and in fact, even higher than the task-related behaviors. This may be due to innate behaviors having common neural information pathways across mice, whereas learnt behaviors may display significant differences across mice.

C. Region-based differences in commonalities

In this work, we studied the following brain regions: Primary somatosensory cortex (SSp), Secondary motor cortex (MOs), Primary motor cortex (MOp), Main olfactory bulb (MOB), and Primary visual cortex (VIS). We see that, surprisingly, the sensory areas such as the visual and the somatosensory areas are much more highly correlated across mice for all behaviors as compared to motor behaviors. This may be due to the similarities in sensory feedback due to these similar behaviors, but is a topic of future exploration.

IV. Discussion

In this work, we study the relations between neural activities while different subjects perform the same task-related and spontaneous behaviors across mice. Historically, this has been difficult to explore because of the difficulties in extracting the same behaviors across mice. Here, we applied a new behavioral analysis tool called CS-VAE to extract across-subject behavioral latents from high-dimensional videos. Having extracted similar behaviors across animals, we studied the neural activity within similar task-related and spontaneous behaviors, and found that both have a high level of correlation across subjects. The level of correlation during both of these behaviors across subjects is much higher than the level of correlation if the mice are idle. During idle behavior, the mice have varied cognitive activity that get entrained when faced with performing a task such as a lever pull. Here, we find that the neural activity across subjects during spontaneous behaviors such as grooming also have a high correlation across mice, which has been under-explored in the past. Our study paves the way for a principled approach toward this quantification.

References

[1] M. Safaie, J. C. Chang, J. Park, L. E. Miller, J. T. Dudman, M. G. Perich, and J. A. Gallego, "Preserved neural population dynamics across animals performing similar behaviour," *bioRxiv*, 2022.

[2] A. Mathis, P. Mamidanna, K. M. Cury, T. Abe, V. N. Murthy, M. Mathis, and M. Bethge, "Deeplabcut: markerless pose estimation of user-defined body parts with deep learning," *Nature Neuroscience*, vol. 21, pp. 1281–1289, 2018.

[3] T. Pereira, D. E. Aldarondo, L. Willmore, M. Kislin, S. S.-H. Wang, M. Murthy, and J. W. Shaevitz, "Fast animal pose estimation using deep neural networks," *bioRxiv*, 2018.

[4] Z. Chen, R. Zhang, Y. Eva Zhang, H. Zhou, H.-S. Fang, R. R. Rock, A. Bal, N. Padilla-Coreano, L. Keyes, K. M. Tye, and C. Lu, "Alphatracker: A multi-animal tracking and behavioral analysis tool," *bioRxiv*, 2020.

[5] A. Wiltschko, M. Johnson, G. Iurilli, R. Peterson, J. Katon, S. Pashkovski, V. Abraira, R. Adams, and S. Datta, "Mapping sub-second structure in mouse behavior," *Neuron*, vol. 88, no. 6, pp. 1121–1135, 2015.

[6] A. B. Wiltschko, T. Tsukahara, A. Zeine, R. Anyoha, W. Gillis, J. E. Markowitz, R. E. Peterson, J. M. Katon, M. J. Johnson, and S. R. Datta, "Revealing the structure of pharmacobehavioral space through motion sequencing," *Nature neuroscience*, vol. 23, pp. 1433 – 1443, 2020.

[7] E. Batty, M. Whiteway, S. Saxena, D. Biderman, T. Abe, S. Musall, W. Gillis, J. Markowitz, A. Churchland, J. P. Cunningham, S. R. Datta, S. Linderman, and L. Paninski, "Behavenet: nonlinear embedding and bayesian neural decoding of behavioral videos," in *Advances in Neural Information Processing Systems* (H. Wallach, H. Larochelle, A. Beygelzimer, F. d'Alché-Buc, E. Fox, and R. Garnett, eds.), vol. 32, Curran Associates, Inc., 2019.

[8] D. Yi, S. Musall, A. Churchland, N. Padilla-Coreano, and S. Saxena, "Disentangled multi-subject and social behavioral representations through a constrained subspace variational autoencoder (cs-vae)," *bioRxiv*, 2022.

[9] M. R. Whiteway, D. Biderman, Y. Friedman, M. Dipoppa, E. K. Buchanan, A. Wu, J. Zhou, N. Bonacchi, N. J. Miska, J.-P. Noel, E. Rodriguez, M. Schartner, K. Socha, A. E. Urai, C. D. Salzman, T. I. B. Laboratory, J. P. Cunningham, and L. Paninski, "Partitioning variability in animal behavioral videos using semi-supervised variational autoencoders," *bioRxiv*, 2021.

[10] S. Saxena, I. Kinsella, S. Musall, S. H. Kim, J. Meszaros, D. N. Thibodeaux, C. Kim, J. Cunningham, E. M. C. Hillman, A. Churchland, and L. Paninski, "Localized semi-nonnegative matrix factorization (locanmf) of widefield calcium imaging data," *PLOS Computational Biology*, vol. 16, pp. 1–28, 04 2020.

[11] P. C. Sharma, R. Raja, S. K. Vishwakarma, S. Sharma, P. K. Mishra, and V. S. Kushwah, "Analysis of brain signal processing and real-time eeg signal enhancement," *Multimedia Tools and Applications*, vol. 81, no. 28, pp. 41013–41033, 2022.

[12] A. Tigrini, M. Scattolini, A. Mengarelli, S. Fioretti, M. Morettini, L. Burattini, and F. Verdini, "Role of the window length for myoelectric pattern recognition in detecting user intent of motion," in *2022 IEEE International Symposium on Medical Measurements and Applications (MeMeA)*, pp. 1–6, 2022.

[13] S. Musall, M. T. Kaufman, A. L. Juavinett, S. Gluf, and A. K. Churchland, "Single-trial neural dynamics are dominated by richly varied movements," *Nature neuroscience*, vol. 22, pp. 1677 – 1686, 2019.

[14] J. Lauer, M. Zhou, S. Ye, W. Menegas, T. Nath, M. M. Rahman, V. Di Santo, D. Soberanes, G. Feng, V. N. Murthy, G. Lauder, C. Dulac, M. W. Mathis, and A. Mathis, "Multi-animal pose estimation and tracking with deeplabcut," *bioRxiv*, 2021.

[15] J. Gallego, M. Perich, R. Chowdhury, S. Solla, and L. Miller, "Long-term stability of cortical population dynamics underlying consistent behavior," *Nature Neuroscience*, vol. 23, pp. 260–270, Feb. 2020.